

Y. DENG¹
J.D. FOWLKES¹
J.M. FITZ-GERALD^{2,✉}
P.D. RACK¹

Combinatorial thin film synthesis of Gd-doped $Y_3Al_5O_{12}$ ultraviolet emitting materials

¹ Dept. of Materials Science and Engineering, The University of Tennessee, Knoxville, TN 37996-2200, USA

² Dept. of Materials Science and Engineering, The University of Virginia, Charlottesville, VA 22904-4745, USA

Received: 12 August 2003/Accepted: 29 September 2003
Published online: ■ ■ 2003 • © Springer-Verlag 2003

ABSTRACT Multi-layer $Y_3Al_5O_{12} : Gd$ thin films were deposited in a combinatorial fashion using radio-frequency magnetron sputtering. Initially, $Y_3Al_5O_{12}$ (yttrium aluminum garnet or YAG) films were deposited in a combinatorial fashion to optimize the Y and Al sputtering conditions. Subsequently, alternating layers of uniform $Y_3Al_5O_{12}$ and graded Gd were deposited and the film composition was homogenized by post-deposition 1000 °C 10-h thermal treatment. A composition range of ~ 1–12 at% Gd was produced in two films. Ultraviolet emission with a peak wavelength at 312 nm was observed from the gadolinium $^8S_{7/2} - ^6P_{7/2}$ transition via cathodoluminescence (CL) excitation. The CL-induced intensity was found to be maximum at ~ 5.5 at% Gd.

PACS ■; ■; ■

Miniaturized ultraviolet (250–350 nm) emitting solid-state sources are necessary components for proposed device structures such as non-line-of-sight communication transceivers and receivers and bio-particle detection units. Previous work on thin film rare earth doped $Y_3Al_5O_{12}$ materials have shown emission from the blue to near infra-red range of the electromagnetic spectrum from trivalent Nd [1, 2], Sm [3], Eu [4, 5], Tb [4, 6, 7], Ce [2, 8, 9]. We have recently examined gadolinium-doped YAG powders which photoluminesce at 312 nm [10]. In this paper we will report work on gadolinium-doped YAG thin films that are being explored as a potential material for thin film solid-state UV device applications.

Gadolinium-doped YAG thin films have been prepared by combinatorial sputtering using a radio-frequency magnetron sputtering system (AJA international, ATC 2000–V). The magnets supporting the sputter targets were operated in an unbalanced mode to maximize the deposition rate. The magnetron system has a “sputter-up” configuration, where the substrate surface is located above three sputter targets that are tilted and facing the substrate. The yttrium and aluminum sources were oriented 180° apart in the chamber and the yttrium and gadolinium guns were oriented 90° in reference to the center of the substrate. All the target centers

are 16.5 cm from the 4" substrate holder center and are tilted at 32 degrees relative to the substrate normal to realize the composition gradients. Figure 1 is a digital photograph of the three-source assembly illustrating the source positions relative to the substrate.

To optimize the $Y_3Al_5O_{12}$ deposition an initial deposition was performed by reactively sputtering the yttrium (80 W) and aluminum (120 W) targets in a mixed Ar (25 sccm) and O_2 (2 sccm) atmosphere (3 mTorr) where the O_2 is injected at the substrate and the Ar is injected at the target to extend the range of the metallic reactive sputtering mode. The initial sputtering powers were estimated from previous Y_2O_3 and Al_2O_3 sputtering rate data to give an Al/Y ratio of 5/3 (= 1.66) in the center of the substrate. Energy dispersive X-ray analysis (EDS) of the annealed film (Fig. 2) reveals that the Al/Y ratio ranged from (4.44 – –0.24) over the 100 mm silicon substrate with stoichiometric composition falling very close to the center. The total cation/anion ratio (Al + Y)/O as a function of position is also plotted in Fig. 2 which is slightly above the stoichiometric ratio of 0.67 and shows that the cation content increases as the yttrium content increases. This is consistent with Y_2O_3 films which we have deposited which have measured cation-to-anion ratios of ~ 0.85.

Subsequent to the pure $Y_3Al_5O_{12}$ film deposition, two gadolinium-doped $Y_3Al_5O_{12}$ films were deposited in a com-



FIGURE 1 Digital photograph of the 3-source configuration for the combinatorial sputter deposition process

✉ Fax: ■, E-mail: jmf8h@virginia.edu

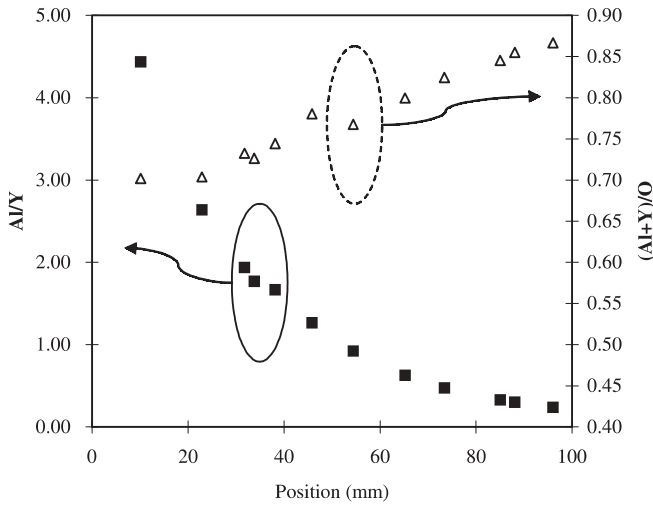


FIGURE 2 EDS results illustrating the Al/Y ratio (right axis) and (Al+Y)/O ratio (left axis) as a function of position on the substrate for the un-doped $Y_3Al_5O_{12}$ sample

binatorial fashion to determine the optimum gadolinium concentration. The combinatorial films were deposited in a multi-layer fashion; a total of seven alternating layers, $Y_3Al_5O_{12} - [Gd - Y_3Al_5O_{12}]_3$ were deposited. To realize a uniform $Y_3Al_5O_{12}$ composition the $Y_3Al_5O_{12}$ layers were deposited in rotation for 12.5 minutes. To realize the gadolinium gradient, the substrate was aligned parallel to the sputter axis of the gadolinium source and deposited with a stationary substrate at 60 W. For the first gadolinium-doped film (Gd-A), each gadolinium layer was sputtered for 4 min and for the second film (Gd-B) each gadolinium layer was sputtered for 8 min. The total film thickness was approximately $1 \mu m$ and varies only slightly due to the variation in the Gadolinium concentration. As will be demonstrated, the concentration gradient, and subsequently the thickness gradient, for Gd-A is on the order of 5% and for Gd-B on the order of 10%. Subsequent to the deposition, the films were annealed at $1000^\circ C$ to homogenize the gadolinium activator throughout the film and crystallize the film. Figure 3 shows a scanning electron

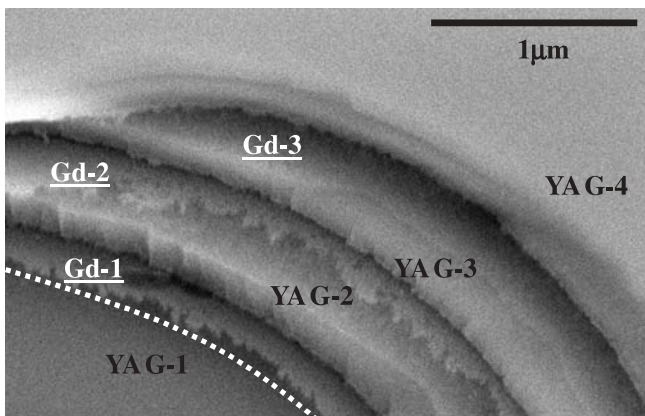


FIGURE 3 Scanning electron micrograph illustrating the discreet $Y_3Al_5O_{12}$ (1-4) and Gd (1-3) layers in the as-deposited film. The $Y_3Al_5O_{12}$ layers are terraced due to the cleaving step and on each layer the thin Gd film can be observed. The dashed white line outlines the first gadolinium layer

micrograph of a cleaved edge of Gd-B prior to the post-deposition annealing step, which shows the discreet $Y_3Al_5O_{12}$ (1, 2, 3, 4) and Gd (1, 2, 3) layers. The $Y_3Al_5O_{12}$ layers are terraced due to the cleaving and on each layer the thin Gd film is observed.

To investigate the crystallinity of the Gd-doped YAG films, $\theta - 2\theta$ X-ray diffraction scans were taken before and after the post deposition anneal. As-deposited films were amorphous, however subsequent to the anneal, the YAG phase was evident with a preferred (420) orientation. EDS measurements of the two films confirmed the uniformity of the yttrium and aluminum content, which has a consistent Al/Y ratio of 1.5. Figure 4 illustrates the Gd composition across the substrate which monotonically increases from ~ 1.5 to 6.3% for Gd-A and ~ 3.5 to 12.5% for Gd-B. The composition range was expected to double for Gd-B relative to Gd-A as the gadolinium sputtering time doubled. The EDS measured cation/anion ratio for the films was also greater than the stoichiometric value of 0.67, and increased with increasing gadolinium content. This is likely due to the fact that the gadolinium layers were metallic rather than oxide films.

To measure the ultraviolet emission of the thin films, cathodoluminescent (CL) measurements were performed in a custom-built vacuum test chamber. The CL measurements were performed at a pressure of $2 \times 10^{-7} - 5 \times 10^{-7}$ Torr at 5 keV beam energy and $\sim 100 \mu A/cm^2$ current density. To confirm that the thickness gradient would not have an effect on the CL measurements a Monte Carlo simulation of 10,000 electrons at 5 keV impinging on $Y_3Al_5O_{12}$ was performed. The electron range or penetration depth of the 5 keV beam on $Y_3Al_5O_{12}$ was determined to be approximately $0.15 \mu m$, which is much shallower than the thinnest sample. CL spectra were measured across the Gd-A and Gd-B substrate with an Ocean Optics PC2000 spectrometer with a pixel integration time of 100 ms. Figure 5a illustrates a typical Gd-doped YAG spectrum which has its dominant peak at 312 nm from the Gd

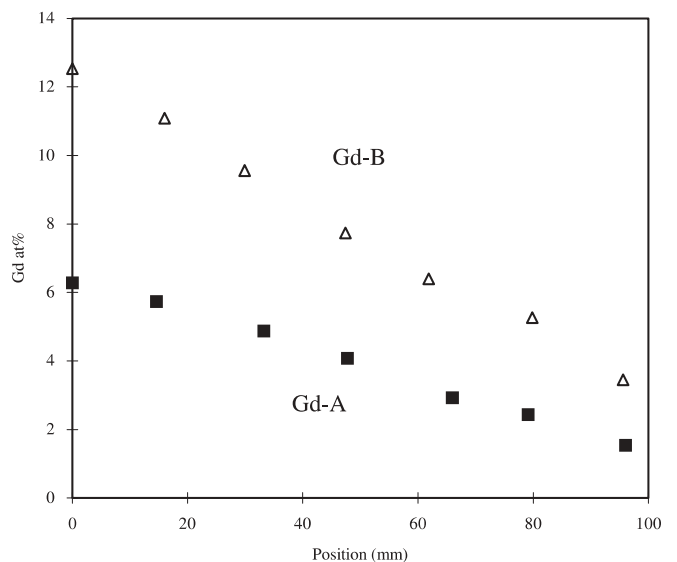


FIGURE 4 Plot of the gadolinium concentration as a function of position for the two (Gd-A and Gd-B) doped $Y_3Al_5O_{12}$ films. A gadolinium composition range of $\sim 1.5\%$ to 6.3% for Gd-A and $\sim 3.5\%$ to 12.5% for Gd-B was achieved

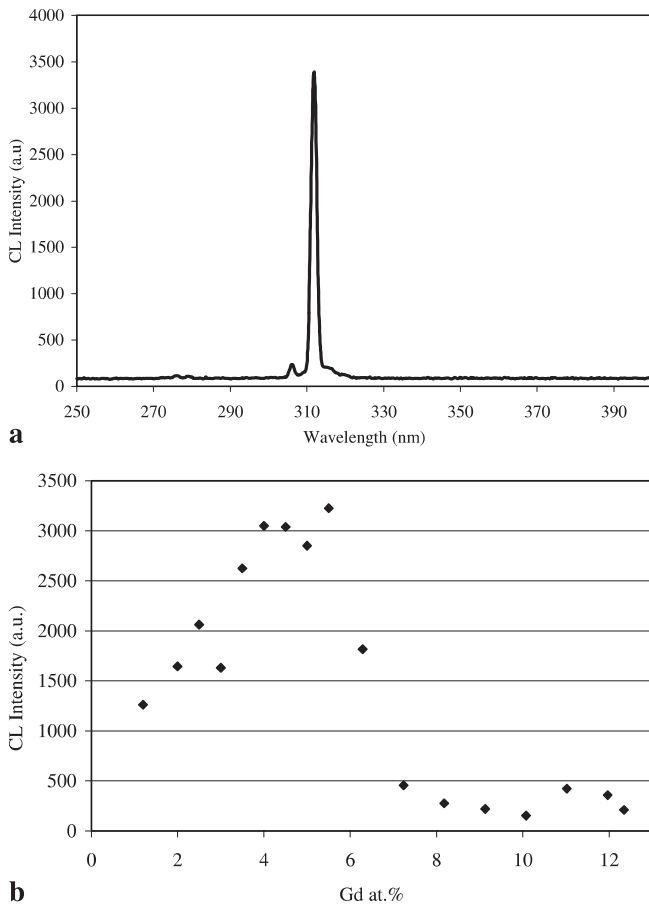


FIGURE 5 **a** Typical gadolinium-doped $Y_3Al_5O_{12}$ cathodoluminescence spectrum illustrating the ultraviolet $^8S_{7/2} - ^6P_{7/2}$ transition. **b** Plot of the CL intensity versus the gadolinium concentration in the two sputter deposited films

$^8S_{7/2} - ^6P_{7/2}$ intrashell $4f - 4f$ transition. Figure 5b shows the normalized CL intensity at 312 nm versus the gadolinium concentration. Overlapping data points (i.e. 3.5%–5.35%) were averaged for the two samples. Figure 5b shows a nearly linear increase in CL intensity with increasing Gd% from 1%–5.5% and a precipitous drop off at concentrations greater than $\sim 5.5\%$.

The $A_3B_5O_{12}$ garnet structures have three cation sites: B tetrahedral and octahedral sites and A dodecahedral sites. For the Gd-doped YAG, the Gd^{3+} dopant occupies the yt-

trium (A) positions in the YAG material due to the similar ionic radii. The nearest neighbor A–A distance in YAG is 0.367 nm [11, 12]. For the trend observed in Fig. 5b, the CL intensity increases with gadolinium concentrations up to $\sim 5.5\%$. In this region, the CL intensity simply increases because there are more activators available for excitation. At gadolinium concentrations greater than $\sim 5.5\%$, the CL intensity quenches. This concentration is in good agreement with Yb-doped YAG films which concentration quench at $\sim 4\%$ [12]. At these high concentrations, the large number of nearest neighbor Gd-Gd sites induce non-radiative energy transfer among the excited state gadolinium activators, which subsequently get recombined at non-radiative centers.

In summary, we have used a combinatorial rf magnetron sputtering method to synthesize gadolinium doped ultraviolet emitting $Y_3Al_5O_{12}$ thin films. An initial deposition was performed to optimize the Al/Y ratio in the $Y_3Al_5O_{12}$ films and two subsequent films were deposited with uniform $Y_3Al_5O_{12}$ and graded Gd layers. EDS and X-ray diffraction confirmed the stoichiometric composition and YAG crystal structure, respectively. Two gadolinium composition ranges were achieved spanning a total composition range of $\sim 1\%$ – 12% gadolinium. CL measurements of the films revealed an optimum concentration at $\sim 5.5\%$ Gd which is in good agreement with other rare earth doped YAG materials.

REFERENCES

- 1 R. Rumianowski, F. Rozploch, R.S. Dygdala, S. Slawomir, P. Plociennik, A. Wojtowicz: *Appl. Surf. Sci.* **193**, 261 (2002)
- 2 M. Ezaki, M. Obara, H. Kurnagai, K. Toyoda: *Appl. Phys. Lett.* **69**, No. 20, 2977 (1996)
- 3 C. Sanchez-Valle, I. Daniel, B. Reynard, R. Abraham, C. Goutaudier: *J. Appl. Phys.* **92**, No. 8, 4349 (2002)
- 4 A. Esparza, M. Garcia, C. Falcoy: *Thin Sol. Films* **325**, 14 (1998)
- 5 D. Ravichandran, R. Roy, A.G. Chakhovskoi, C.E. Hunt, W.B. White, S. Erdei: *J. Lumin.* **71**, 291 (1997)
- 6 G.A. Hirata, O.A. Lopez, L.E. Shea, J.Y. Yi, T. Cheeks, J. McKittrick, J. Siqueiros, M.A. Borja, A. Esparza, C. Falcoy: *J. Vac. Sci. Technol. A* **14**, No. 3, 1694 (1996)
- 7 J.Y. Choe, D. Ravichandran, S.M. Blomquist, D.C. Morton, K.W. Kirchner, M.H. Ervin, U. Lee: *Appl. Phys. Lett.* **78**, No. 24, 3800 (2001)
- 8 C.H. Lu, H.C. Hong, R. Jagannathan: *J. Mat. Sci. Lett.* **21**, 1489 (2002)
- 9 J.Y. Choe: *Mat. Res. Innovat.* **6**, 238 (2002)
- 10 unpublished with Steve Allison at Oak Ridge National Laboratories
- 11 E. Antic-Fidancev, J. Holsa, M. Lastusaari, A. Lupei: *Phys. Rev. B* **64**, 195 108-1-8 (2001)
- 12 G. Boulon, L. Laversenne, C. Goutaudier, Y. Guyot, M.T. Cohen-Adad: *J. Lumin.* **102–103**, 417 (2003)